Effect of Plastic Type and Salt Concentration on Interactions Between Nanoscale Plastic and Amino Acids in Solution using Saturation-Transfer Difference NMR Spectroscopy

Rajan Rai, Ashley A. Abel, and Leah B. Casabianca*

Department of Chemistry, Clemson University, Clemson, SC, 29634, USA

Abstract

We have used Saturation-Transfer Difference NMR (STD-NMR) spectroscopy to examine binding between amino acids and nanoparticles that are composed of different kinds of plastic. We have also examined how the presence of salt influences these interactions. We find that the presence of salt decreases binding that is primarily due to electrostatic interactions. Additionally, phenylalanine binding to polyethylene and polypropylene nanoparticles is negligible as compared to binding to polystyrene nanoparticles. Lysine and leucine exhibit binding to polypropylene nanoparticles, and this binding is due to electrostatic interactions. Last, we have shown that these experiments can be done in natural water samples including lake and river water, by adding a minimal amount of D_2O to the natural water. The results of these studies can be applied to understanding the fundamental interactions that are responsible for binding between nanoplastic and biological macromolecules or between nanoplastic and small molecule xenobiotics. This work has implications in the study of nanoscale plastic pollution, as nanoscale plastic pollution can absorb toxic small molecule contaminants in the environment.

*corresponding author, lcasabi@clemson.edu

Keywords: microplastic, nanoplastic, polystyrene, polyethylene, polypropylene, amino acids, nanoparticle, binding, STD-NMR

Synopsis: Micro- and nanoscale plastic in the environment interacts with small molecules with myriad consequences for environmental health.

Introduction

Increasing production and use of plastics is one of the major current contributors to environmental pollution.[1-5] Large plastic particles are thought to degrade into smaller particles,[6] approaching the micro and nano scale. Factors such as exposure to UV light, fouling by microorganisms, exposure to high salt concentrations in seawater, and mechanical weathering can affect the rate of plastic degradation[7] and plastic nanoparticle formation.[8] Plastic microparticles have been found almost everywhere, from Mt. Everest[9] to the Mariana Trench.[10]

Exposure to micro- and nanoscale plastic has been shown to cause a variety of toxicological effects including inflammation,[11] DNA damage,[12] behavioral disorders,[13] decreased reproduction,[11] and brain damage[13] in aquatic life and placental disruption in mice.[14] Mitochondrial damage was also observed in human cells upon exposure to plastic nanoparticles.[15]

In addition to the negative effects associated with the plastic nanoparticles themselves, these small plastic particles can adsorb or absorb and transport other contaminants such as pesticides,[16] herbicides,[17,18] heavy metals,[19] and pharmaceuticals.[16,20,21] Since nano-scale plastic has been shown to travel through the food chain[12,13] and has been found in commercial sea salt[22] and commercial beverages,[23] toxicity of nanoplastics and transport of toxins by plastic nanoparticles is a concern for human health as well. Sorption of small molecules by nanoparticles is presumably dictated by the nanoparticle surface functionality. Unfortunately, the nature of the surface of micro- and nanoscale plastic in the environment can vary and is largely unknown.[24] Therefore, there is a need to develop methods to understand how small molecules are taken up by micro- and nanoscale plastic particles in an aqueous environment. There is also a need to understand how other molecules that are also present in natural water, such as various kinds of salt, influence these interactions.

Previously, we[21,25-29] and others[30-36] have used Saturation-Transfer Difference (STD)-NMR to study binding between small molecules and nanoparticles. STD-NMR is one of several NMR-based approaches to studying interactions between small molecules and nanoparticles.[37-39] Another popular method is dark-state exchange saturation transfer (DEST), which can also be applied to non-protonated nanoparticles.[40,41] The STD-NMR experiment[42,43] can be used to rapidly identify small molecules that bind to a large receptor, even in the presence of non-binding molecules. The STD-NMR experiment consists of collecting two NMR spectra. In the first spectrum, called the on-resonance spectrum, the receptor is selectively saturated before the NMR experiment by applying radiofrequency irradiation at a frequency at which only the receptor resonates. This saturation is then transferred to any small molecule ligand that is associated with the receptor surface during the saturation time, and saturation of the ligand results in a decrease in the intensity of the ligand NMR signal. Signals from small molecules that do not bind to the receptor, on the other hand, will not receive any saturation transfer, so their NMR signals will not change in intensity. In the second spectrum, called the off-resonance spectrum, saturation is performed at the same power and for the same amount of time, but at a frequency that is far from both the receptor and ligand resonances. This saturation should not disturb either the ligand or the receptor, so the off-resonance spectrum is essentially a reference spectrum. The STD difference spectrum is then constructed by subtracting the on-resonance spectrum from the off-resonance spectrum. Since non-binding ligands will have the same signal intensity in the on- and off-resonance spectrum, the difference spectrum will consist of only signals from those ligands that interact with the receptor during the saturation time. The STD effect is then defined as the STD difference intensity divided by the reference intensity.[42]

The advantage of the STD-NMR approach as compared to standard methods to study binding, such as adsorption isotherms, is that it provides site-specific information that can be used for epitope mapping.[42] In other words, the STD-NMR technique can tell us which part of the molecule

is responsible for binding. The amount of saturation transfer to the bound ligand depends on the distance of the observed nucleus to the receptor surface, so nuclei with a larger STD effect are closer to the receptor surface in the bound configuration. This epitope-mapping capability of STD-NMR has been used by us in the past to show that polystyrene nanoparticles can sorb aromatic amino acids through pi-pi interactions, charged amino acids through electrostatic effects, and long-chain aliphatic amino acids through London dispersion interactions.[25,27]

Here, we extend these studies to other types of plastic, namely polyethylene and polypropylene.[2] Additionally, we embark on a systematic study of the influence of different kinds of salt (NaCl, $CaCl_2$, and $MgSO_4$) on interactions between nanoparticles and small molecules. As in the previous studies, amino acids are used as model small molecules since they contain a variety of functional groups. Amino acids are also the building blocks of proteins, so insight into amino acid interactions with nanoparticle surfaces can be extrapolated to predict interactions that are responsible for binding between plastic nanoparticles and biological macromolecules. These interactions are responsible for formation of the nanoparticle protein corona, cellular uptake of nanoparticles, and other phenomena that occur at the nano-bio interface.[44] The study of amino acids binding to plastic nanoparticles will also lead to fundamental knowledge about the driving forces that are responsible for binding, and this knowledge can then be applied to larger, more complicated molecules such as antibiotics.[21]

Methods

Carboxylate-modified nanoparticles were used for the experiments. Polystyrene latex beads (45 nm, 4% w/v) were purchased from Thermo Fisher Scientific (Waltham, MA) and polypropylene (53.6 nm, 1% solids) and polyethylene (64.9 nm, 1% solids) microparticles were purchased from Lab261 (Palo Alto, CA). Amino acids (D-phenylalanine, L-lysine, L-leucine, and L-glutamic acid), sodium chloride, calcium chloride dihydrate, and magnesium sulfate heptahydrate were purchased from Sigma-Aldrich (St. Louis, MO). Deuterium oxide (D, 99.9%) was purchased from Cambridge Isotope Laboratories Inc. (Tewksbury, MA) and deionized water was purified using a RiOs-DI® 3 system by MilliporeSigma (Burlington, MA).

Stock solutions of amino acids and salts were prepared by dissolving their calculated amounts in D_2O or D_2O/H_2O mixtures. Stock solutions of amino acids, salts, and/or nanoparticle suspensions were then combined for the final samples. The final samples consisted of 10 mM amino acids, various concentrations of polystyrene nanoparticles (PSNP), polyethylene nanoparticles (PENP), or polypropylene nanoparticles (PPNP), and different concentrations of salt as listed in the relevant figure captions. All samples had a final D_2O:H_2O ratio of 71:29 (v/v). Samples (0.5 mL each) were transferred to 5 mm NMR tubes (Bruker Biospin, Inc, Billerica, MA) after mixing sufficiently.

All NMR experiments were run on a Bruker Avance NEO 500 MHz spectrometer with a Prodigy nitrogen-cooled CryoProbe. The 90° pulse length was calibrated for each sample and ranged from 11.90 μs to 15.95 μs. The standard pulse sequence “stddiffesgp” was used for the STD NMR experiments.[42,43] Saturation was performed at the frequencies of -1 ppm (on-resonance) and 40 ppm (off-resonance). A range of saturation times was selected from 0.1 to 10.0 seconds. Each experiment was acquired with a 16.38 ppm spectral width, 2 s acquisition time, 4 dummy scans, 16 scans, and a relaxation delay of 12 s. For water peak suppression, the excitation sculpting with gradients water suppression sequence was employed.[45] All experiments were carried out at a temperature of 298 K. NMR spectra were processed with Bruker Topspin software (Topspin 4.3.0 or 4.1.4) and the peak integrals were calculated using MATLAB R2023a software (The MathWorks Inc., Natick, MA).

An Accumet AB150 pH meter (Fisher Scientific) was used for the pH measurement of the samples. The pH reported is that which was read directly from the pH meter, without correction for isotope effects.

The average particle sizes of the samples were determined by dynamic light scattering (DLS) using a NanoBrook Omni particle sizer (Brookhaven Instruments, Holtsville, KY). Five experiments were performed on each sample. The scattering angle used was 90°. Each measurement lasted 180 seconds, with 180 seconds of sample equilibration and a 10 second delay between each measurement. Zeta potential measurements were made using the Smoluchowski method, with 30 run cycles, a 10-second inter-cycle delay, and 240 second equilibration time. All experiments were carried out at 25°C. For DLS, 40 μL of each NMR sample was added to 3 mL of H_2O and for zeta potential measurements, 2.5 μL of PSNP or 10 μL of PENP or PPNP were diluted to 1.5 mL total in order to have concentrations that are appropriate for DLS or zeta potential measurements.

Results and Discussion

Figure 1 shows the 1D proton NMR spectra of the four amino acids studied. Their proton peaks were assigned with the assistance of the Human Metabolome Database[46] and Biological Magnetic Resonance Data Bank.[47]

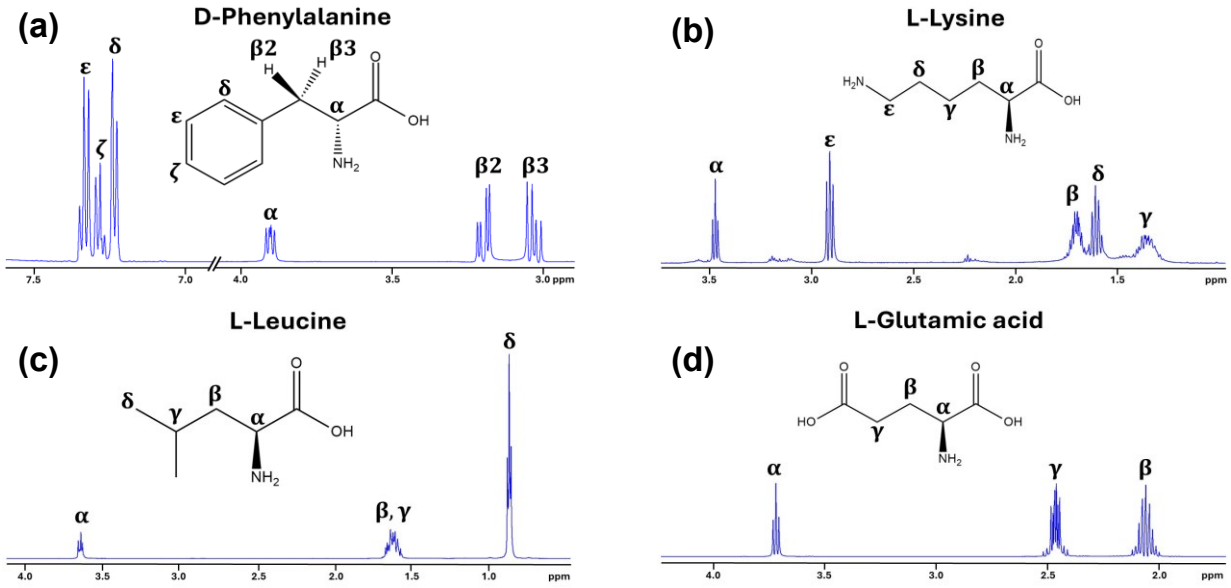

Figure 1. 1D proton NMR spectra and peak assignments for (a) phenylalanine, (b) lysine, (c) leucine, and (d) glutamic acid.

STD buildup curves for phenylalanine, lysine, leucine, and glutamic acid in the presence of PSNP are shown in Figure 2. In addition, STD buildup curves are also shown for these four amino acids in the presence of PSNP and various salts that may be expected to be present in seawater. The four amino acids were chosen as examples of aromatic (Phe), positively-charged (Lys), aliphatic (Leu), and negatively-charged (Glu) amino acids. In previous work,[27] we found that phenylalanine, lysine, and leucine interacted with PSNP with decreasing binding strength through pi-pi interactions, electrostatic effects, and London dispersion interactions, respectively. Glutamic acid was not observed to interact with negatively-charged PSNP, as it is also negatively charged at

neutral pH. The results shown in Figure 2 (a), (e), (i), and (m) agree with these findings, even though these were performed without buffer and the pH of the glutamic acid samples is near the pI of Glu. Representative STD reference and difference spectra are shown in the supporting information in Figure S1.

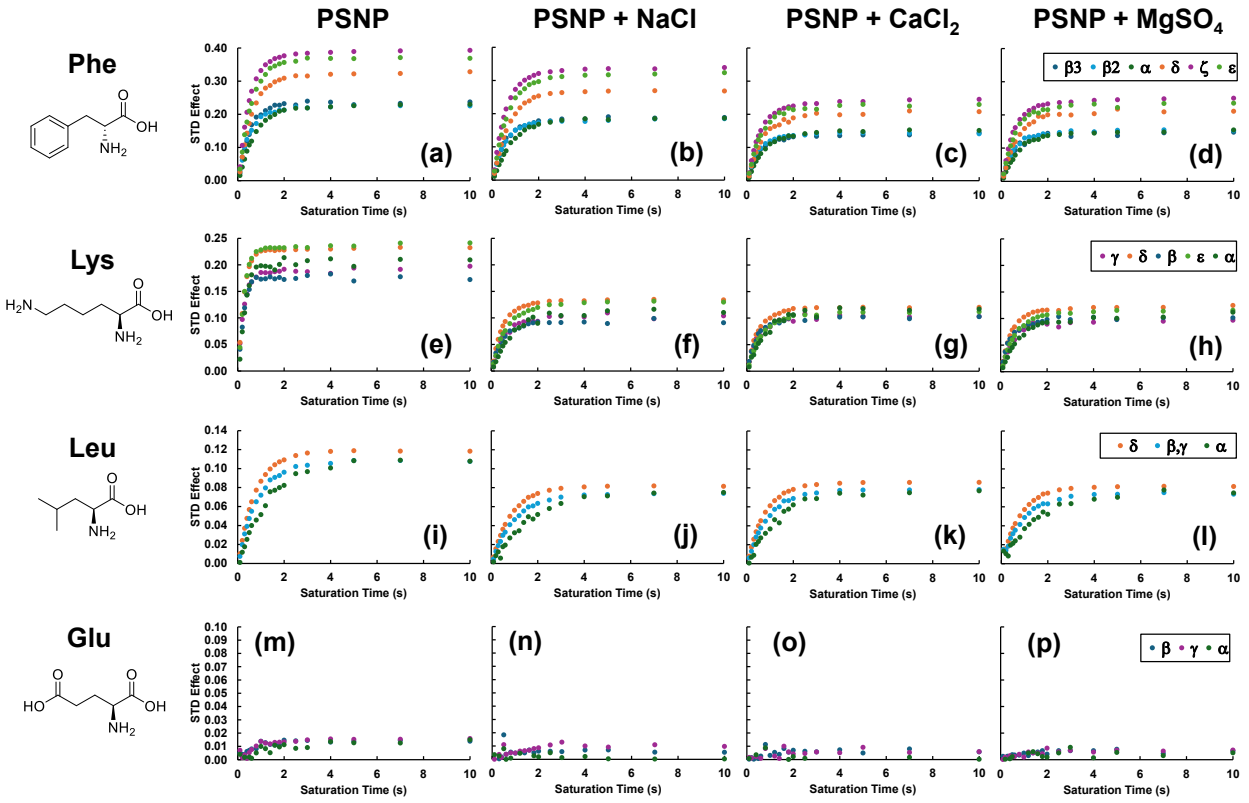

Figure 2. STD buildup curves for amino acids phenylalanine (Phe), lysine (Lys), leucine (Leu), and glutamic acid (Glu), each at a concentration of 10 mM, interacting with 264 nM PSNP in the absence of salt and in the presence of 75 mM NaCl, 25 mM $CaCl_2$, or 18.75 mM $MgSO_4$. (a) Phe+PSNP, (b) Phe+PSNP+NaCl, (c) Phe+PSNP+$CaCl_2$, (d) Phe+PSNP+$MgSO_4$, (e) Lys+PSNP, (f) Lys+PSNP+NaCl, (g) Lys+PSNP+$CaCl_2$, (h) Lys+PSNP+$MgSO_4$, (i) Leu+PSNP, (j) Leu+PSNP+NaCl, (k) Leu+PSNP+$CaCl_2$, (l) Leu+PSNP+$MgSO_4$, (m) Glu+PSNP, (n) Glu+PSNP+NaCl, (o) Glu+PSNP+$CaCl_2$, (p) Glu+PSNP+$MgSO_4$. Greek letters in the legend identify the proton of the amino acid according to IUPAC recommendations,[48] as shown in Figure 1.

As can be seen from the remaining panels in Figure 2, the presence of either of the three salts tested decreases the STD effect of Phe, Lys, and Leu in the presence of PSNP. This is to be expected if at least some PSNP-amino acid interaction is attributed to electrostatic effects between these amino acids and the negatively-charged PSNP in each case. The presence of salt then screens the charges and decreases the extent of binding due to electrostatic effects. The salt concentrations in Figure 2 were chosen so that all samples have the same ionic strength (μ = 75 mM). From Figure 2, the effect of salt on leucine and lysine binding to PSNP appears to be related to the ionic strength, rather than on the identity of the salt. In the case of phenylalanine, binding is disrupted more by the divalent salts than by NaCl. Glutamic acid, which is negatively charged at physiological pH, exhibits negligible STD effects in the presence of PSNP, and this is not changed by the presence of salt. We initially hypothesized that salt may screen the negative

charges between Glu and PSNP such that the two can interact, leading to an observable STD effect. However, based on the buildup curves in Figure 2 (m-p), this was not seen to be the case.

To model salt concentrations that are closer to that found in seawater, we have repeated the experiments with 600 mM NaCl. The results are shown in Figure 3. The STD buildup curves with higher salt concentration follow the same trends as those in Figure 2 – the STD effects for phenylalanine and lysine decrease with higher salt concentration. The buildup curve for leucine is similar in the presence of 75 mM and 600 mM NaCl. Last, glutamic acid does not exhibit appreciable STD effects in the presence of PSNP with either 75 mM or 600 mM NaCl. These results indicate that the STD experiment can be carried out in high salt concentrations comparable to the concentration of NaCl in seawater.

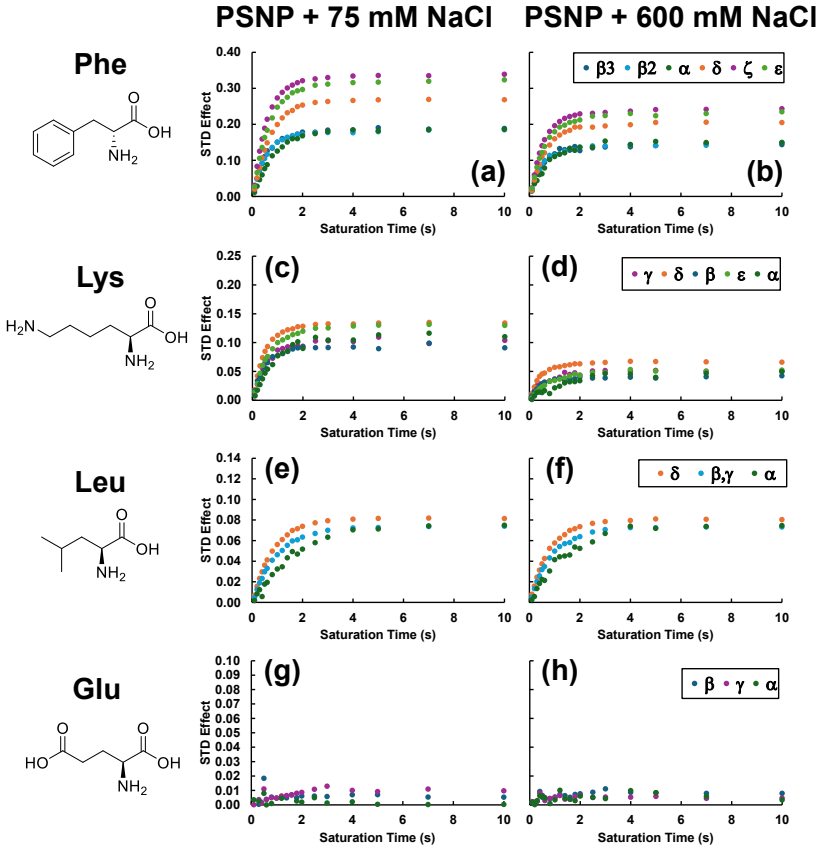

Figure 3. STD buildup curves for phenylalanine, lysine, leucine, and glutamic acid (each at a concentration of 10 mM) interacting with 264 nM PSNP in the presence of either 75 mM or 600 mM NaCl. (a) Phe+PSNP+75 mM NaCl, (b) Phe+PSNP+600 mM NaCl, (c) Lys+PSNP+75 mM NaCl, (d) Lys+PSNP+600 mM NaCl, (e) Leu+PSNP+75 mM NaCl, (f) Leu+PSNP+600 mM NaCl, (g) Glu+PSNP+75 mM NaCl, (h) Glu+PSNP+600 mM NaCl. Greek letters in the legend identify the proton of the amino acid according to IUPAC recommendations,[48] as shown in Figure 1.

The decrease in STD effect upon addition of salt can be attributed to salt disrupting binding through electrostatic interactions, but salt can also cause aggregation of these nanoparticles by screening negative charges on adjacent nanoparticle surfaces. As shown in Figure 4, $CaCl_2$ and $MgSO_4$ cause an increase in the average particle size observed by DLS, indicating that the particles are aggregating. Aggregation of nanoparticles decreases the overall surface area that is available for amino acid binding.

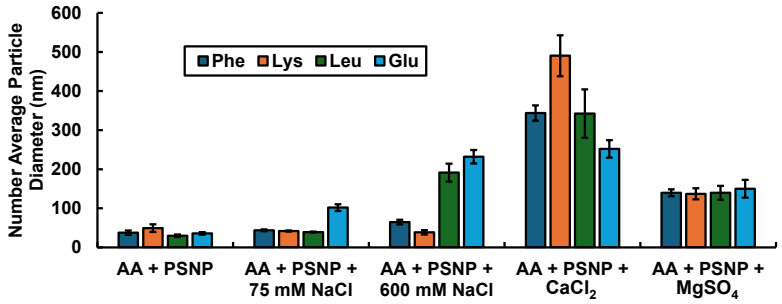

Figure 4. Average particle size from DLS for samples containing amino acids (AA), PSNP, and various concentrations of different salts. Each sample was diluted by a factor of 76 for the DLS measurement; reported concentrations are original salt concentrations for ease of comparison with Figures 2 and 3.

The pH of each sample is listed in Table 1. As these samples were made without buffer, the pH can vary among samples. The pH appears to be determined by the amino acid and addition of salt does not generally drastically change the pH. The pH changes listed in Table 1 are not expected to change the protonation state of any of the amino acids. Also, there is no correlation between pH and the propensity of the PSNP to aggregate.

Table 1. Measured pH values for samples of 10 mM amino acids, 264 nM PSNP, and various concentrations of different salts.

	PSNP	**PSNP + NaCl (75 mM)**	**PSNP + NaCl (600 mM)**	**PSNP + $CaCl_2$ (25 mM)**	**PSNP + $MgSO_4$ (18.75 mM)**
Phe	4.70	4.44	3.90	4.29	4.36
Lys	8.61	8.15	7.33	7.45	7.13
Leu	5.82	4.45	3.89	4.23	4.44
Glu	3.45	3.32	3.16	3.41	3.43

Figure 5 presents STD buildup curves for the amino acids phenylalanine, lysine, and leucine interacting with carboxylate-functionalized nanoparticles that are composed of different kinds of plastic. Polyethylene (PE) and polypropylene (PP) were chosen since they, along with polystyrene, are among the most prevalent polymers that are found in plastic pollution.[2] Since glutamic acid exhibited negligible binding to PSNP in the absence or presence of salt, it was not considered in the comparison of binding among different kinds of plastic.

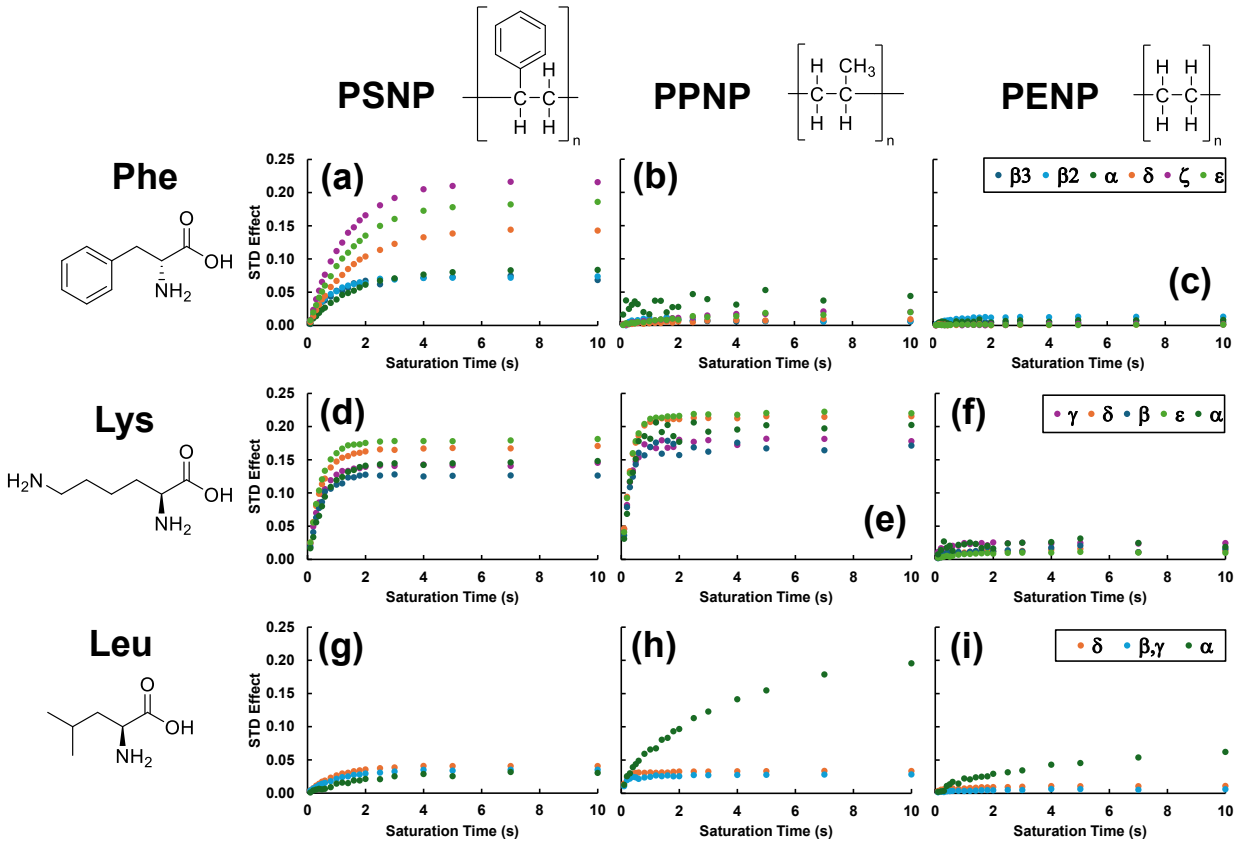

Figure 5. STD buildup curves for phenylalanine, lysine, and leucine (each at a concentration of 10 mM) in the presence of 53 nM polystyrene nanoparticles (PSNP), 44 nM polypropylene nanoparticles (PPNP), or 25 nM polyethylene nanoparticles (PENP). (a) Phe+PSNP, (b) Phe+PPNP, (c) Phe+PENP, (d) Lys+PSNP, (e) Lys+PPNP, (f) Lys+PENP, (g) Leu+PSNP, (h) Leu+PPNP, (i) Leu+PENP. Greek letters in the legend identify the proton of the amino acid according to IUPAC recommendations,[48] as shown in Figure 1.

Figure 5 (a), (d), and (g) show STD buildup curves for Phe, Lys, and Leu in the presence of PSNP, albeit at a lower PSNP concentration than in Figure 2, so that these buildup curves can be compared to those in the presence of PPNP and PENP, which are available commercially only at lower concentrations. As can be seen in Figure 5 (b) and (c), phenylalanine does not exhibit significant STD effects in the presence of either PPNP or PENP. This is to be expected as the main driving force for polystyrene binding to PSNP is thought to be pi-pi interactions, and polypropylene and polyethylene do not contain aromatic groups. These results validate our hypothesis, presented in previous papers,[27,25] that aromatic interactions are primarily responsible for phenylalanine binding to PSNP. In order to show that these kinds of experiments can be carried out in natural water samples, we have repeated the experiments shown in Figure 5 in lake and river water, with a minimum amount of D_2O added for spectrometer lock. The results are shown in the supporting information in Figures S2-S4.

Examining the STD effect at a single saturation time may not be an effective way to measure the relative binding strength, as there are other contributing factors such as nuclear relaxation time and rebinding of the ligand.[49,50] Instead, it has been pointed out that the initial slope of the STD buildup curve can be a more effective measure to assess the relative binding affinity between different ligand-receptor pairs.[50] Therefore, we have calculated the initial slope of the buildup

curves in Figure 5 and displayed them in Figure 6. When interacting with PSNP, the initial slopes of the STD buildup curve are similar for phenylalanine and lysine, and lower for leucine.

STD effects and initial slopes for lysine and leucine actually increase going from PSNP to PPNP. The main driving forces for interaction in both cases are expected to be electrostatic effects and London dispersion forces, so a drastic change in binding strength between polystyrene and polypropylene is not expected. It may be that the carboxylate groups on the surface of the PPNP and PSNP are slightly different, as these nanoparticles come from different manufacturers. The measured zeta potential of the PSNP, PPNP, and PENP are -39 ± 4 mV, -58 ± 3 mV, and -44 ± 1 mV, respectively. In the case of leucine, small STD effects are observed in the presence of PSNP and PPNP, indicating weak but observable interactions. Interestingly, the α proton of leucine exhibits a substantial STD effect in the presence of PPNP, approaching the STD effect of phenylalanine and lysine in the presence of PSNP. There is some overlap between this proton and peaks from the PPNP and PENP, but control experiments done on PPNP and PENP in the absence of leucine indicates that the STD difference is coming from the leucine peak, not the nanoparticle peak. The α proton of leucine is near the charged groups of this amino acid, so this large STD effect may again indicate that electrostatic effects are important to binding these PPNP from Lab261. From the initial slope of the STD buildup curves shown in Figure 6, this large STD effect does not come with a concomitant increase in initial slope. The α proton of leucine has the same relative initial slope compared to the to the other leucine peaks in the presence of PSNP and PPNP.

Neither of the three amino acids studied show significant STD effects in the presence of PENPs. The STD effects in Figure 5 (c), (f), and (i), with the exception of the Leu α proton, are essentially noise. Polyethylene contains fewer methyl groups than polypropylene so would be expected to have the weakest London dispersion interactions with either of the amino acids studied. Again, there might be slight differences in the nature of the carboxylate groups between PPNP and PENP, which may explain why no amino acids seem to be interacting strongly with PENP through electrostatic interactions.

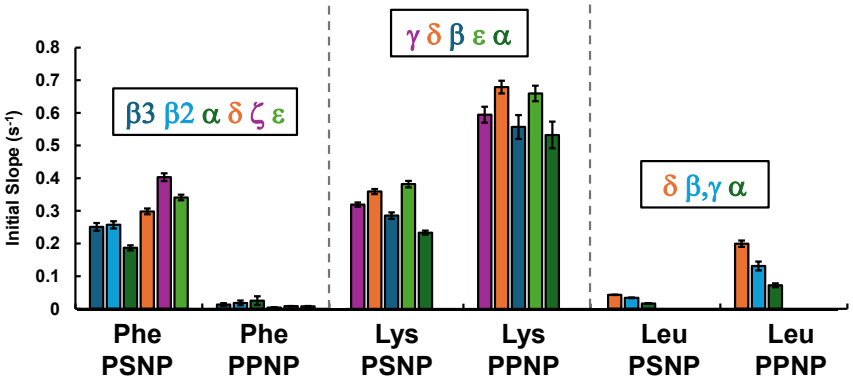

Figure 6. Initial slope of the STD buildup curve for phenylalanine, lysine, and leucine interacting with PSNP and PPNP. The slopes were determined from the buildup curves in Figure 5 (a-b), (d-e), and (g-h). Greek letters in the legend identify the proton of the amino acid according to IUPAC recommendations,[48] as shown in Figure 1.

Conclusions

In this work, we have used STD-NMR to investigate the binding between amino acids phenylalanine, lysine, leucine, and glutamic acid and plastic nanoparticles composed of polystyrene, polypropylene, and polyethylene in the presence and absence of salts that are present in seawater. As expected, binding is strongest between phenylalanine and polystyrene nanoparticles, since pi-pi interactions between phenylalanine and the aromatic group of styrene contribute to binding. Lysine and leucine also interact with PSNP and PPNP through electrostatic effects and hydrophobic interactions, the first of which are disrupted by the presence of salt in the sample. No significant binding is observed to PENP, which is expected to have the lowest capacity for London dispersion interactions with amino acids. However, when interacting with PPNP and PENP, the α proton of leucine exhibits STD effects that are significantly higher than those for other protons of leucine, indicating that the charged part of the leucine molecule is closest to the nanoparticle surface and is therefore responsible for binding. Experiments done at high salt concentrations (600 mM NaCl) indicate that STD-NMR experiments can be performed at salt concentrations that are similar to those in natural seawater. Experiments were also performed in natural lake and river water samples.

Studying the influence of salts on the binding between nanoplastics and biomolecules can be useful to understand the actual picture of what is happening in natural waterways such as seas and oceans. In addition, this work represents our first use of STD-NMR to examine binding between small molecules and plastic nanoparticles that are composed of polyethylene and polypropylene, which are important contributions to nanoscale plastic pollution in the environment.

Supporting Information: Representative STD spectra and STD buildup curves for experiments done in natural water samples.

Acknowledgements

This work was supported by the National Science Foundation (Grants CHE-2304888, CHE-1751529, and CHE-1725919). RR acknowledges support from the Clemson Science Student Advisory Board Grant in Aid of Research. We thank Sekinah Dauda for help with the zeta potential measurements.

References

1. Andrady, J. L.; Neal, M. A. Applications and Societal Benefits of Plastics, *Phiols. T. Roy. Soc. B* **2009**, *364*, 1977-1984.

2. Sharma, V. K.; Ma, X.; Guo, B.; Zhang, K. Environmental Factors-Mediated Behavior of Microplastics and Nanoplastics in Water: A Review, *Chemosphere* **2021**, *271*, 129597.

3. Geyer, R.; Jambeck, J. R.; Law, K. L. Production, use, and fate of all plastics ever made, *Sci. Adv.* **2017**, *3*, e1700782.

4. Walker, T. R.; Fequet, L. Current trends of unsustainable plastic production and micro(nano) plastic pollution, *TRAC-Trend. Anal. Chem.* **2023**, *160*, 116984.

5. Cózar, A.; Echevarría, F.; Ignacio González-Gordillo, J. Irigoien, X.; Ubeda, B.; Hernández-León, S.; Palma, A. T.; Navarro, S.; García-de-Lomas, J.; Ruiz, A.; Fernández-de-Puelles, M. L.; Duarte, C. M. Plastic Debris in the Open Ocean, *Proc. Natl. Acad. Sci. USA* **2014**, *111*, 10239-10244.

6. Barnes, D. K. A.; Galgani, F.; Thompson, R. C.; Barlaz, M. Accumulation and fragmentation of plastic debris in global environments, *Phiols. T. Roy. Soc. B* **2009**, *364*, 1985-1998.

7. O'Brine, T.; Thompson, R. C. Degradation of plastic carrier bags in the marine environment, *Mar. Pollut. Bull.* **2010**, *60*, 2279-2283.

8. Lambert, S.; Sinclair, C. J.; Bradley, E. L.; Boxall, A. B. A. Effects of environmental conditions on latex degradation in aquatic systems, *Sci. Total Environ.* **2013**, *447*, 225-234.

9. Napper, I. E.; Davies, B. F. R.; Clifford, H.; Elvin, S.; Koldewey, H. J.; Mayewski, P. A.; Miner, K. R.; Potocki, M.; Elmore, A. C.; Gajurel, A. P.; Thompson, R. C. Reaching New Heights in Plastic Pollution- Preliminary Findings of Microplastics on Mount Everest, *One Earth* **2020**, *3*, 621-630.

10. Jamieson, A. J.; Brooks, L. S. R.; Reid, W. D. K.; Piertney, S. B.; Narayanaswamy, B. E.; Linley, T. D. Microplastics and synthetic particles ingested by deep-sea amphipods in six of the deepest marine ecosystems on Earth, *Roy. Soc. Open Sci.* **2019**, *6*, 180667.

11. Marana, M. H.; Poulsen, R.; Thormar, E. A.; Clausen, C. G.; Thit, A.; Mathiessen, H.; Jaafar, R.; Korbut, R.; Hansen, A. M. B.; Hansen, M.; Limborg, M. T.; Syberg, K.; Jorgensen, L. v G. Plastic nanoparticles cause mild inflammation, disrupt metabolic pathways, change the gut microbiota and affect reproduction in zebrafish: A full generation multi-omics study, *J. Hazard. Mater.* **2022**, *424*, 127705.

12. Afrose, S.; Tran, T. K. A.; O'Connor, W.; Pannerselvan, L.; Carbery, M.; Fielder, S.; Subhaschandrabose, S.; Palanisami, T. Organ-specific distribution and size-dependent toxicity of polystyrene nanoplastics in Australian bass (*Macquaria novemaculeata*), *Environ. Pollut.* **2023**, *341*, 122996.

13. Mattsson, K.; Johnson, E. V.; Malmendal, A.; Linse, S.; Hansson, L.-A.; Cedervall, T. Brain damage and behavioural disorders in fish induced by plastic nanoparticles delivered through the food chain, *Sci. Rep.* **2017**, *7*,11452.

14. Dibbon, K. C.; Mercer, G. V.; Maekawa, A. S.; Hanrahan, J.; Steeves, K. L.; Ringer, L. C. M.; Simpson, A. J.; Simpson, M. J.; Baschat, A. A.; Kingdom, J. C.; Macgowan, C. K.; Sled, J. G.; Jobst, K. J.; Cahill, L. S. Polystyrene micro- and nanoplastics cause placental dysfunction in mice. *Biol. Reprod.* **2023**, *110*, 211-218.

15. Lin, S.; Zhang, H.; Wang, C.; Su, X.-L.; Song, Y.; Wu, P.; Yang, Z.; Wong, M.-H.; Cai, Z.; Zheng, C. Metabolomics Reveal Nanoplastic-Induced Mitochondrial Damage in Human Liver and Lung Cells, *Environ. Sci. Technol.* **2022**, *56*, 12483-12493.

16. Barreto, M.; Lopes, I.; Oliveira, M. Micro(nano)plastics: A review on their interactions with pharmaceuticals and pesticides, *TRAC-Trend. Anal. Chem.* **2023**, *169*, 117307.

17. Magrì, D.; Veronesi, M.; Sánchez-Moreno, P.; Tolardo, V.; Bandiera, T.; Pompa, P. P.; Athanassiou, A.; Fragouli, D. PET nanoplastics interactions with water contaminants and their impact on human cells, *Environ. Pollut.* **2021**, *271*, 116262.

18. Zhang, Q.; Qu, Q.; Lu, T.; Ke, M.; Zhu, Y.; Zhang, M.; Zhang, Z.; Du, B.; Pan, X.; Sun, L.; Qian, H. The combined toxicity effect of nanoplastics and glyphosate on Microcystis aeruginosa growth, *Environ. Pollut.* **2018**, *243*, 1106-1112.

19. Blancho, F.; Davranche, M.; Marsac, R.; Léon, A.; Dia, A.; Grassl, B.; Reynaud, S.; Gigault, J. Metal-binding processes on nanoplastics: rare earth elements as probes, *Environ. Sci.-Nano* **2022**, *9*, 2094-2103.

20. Almeida, M.; Martins, M. A.; Soares, A. M. V.; Cuesta, A.; Oliveira, M. Polystyrene nanoplastics alter the cytotoxicity of human pharmaceuticals on marine fish cell lines, *Environ. Toxicol. Phar.* **2019**, *69*, 57-65.

21. Arachchi, S. S.; Palma, S. P.; Sanders, C. I.; Xu, H.; Ghosh Biswas, R.; Soong, R.; Simpson, A. J.; Casabianca, L. B. Binding Between Antibiotics and Polystyrene Nanoparticles Examined by NMR, *ACS Environmental Au* **2023**, *3*, 47-55.

22. Ruan, X.; Ao, J.; Ma, M.; Jones, R. R.; Liu, J.; Li, K.; Ge, Q.; Xu, G.; Liu, Y.; Wang, T.; Xie, L.; Wang, W.; You, W.; Wang, L.; Valev, V. K.; Ji, M.; Zhang, L. Nanoplastics Detected in Commercial Sea Salt, *Environ. Sci. Technol.* **2024**, *ASAP Article.*

23. Socas-Hernández, C.; Miralles, P.; González-Sálamo, J.; Hernández-Borges, J.; Coscollà, C. Assessment of anthropogenic particles content in commercial beverages, *Food Chem.* **2024**, *447*, 139002.

24. Peller, J. R.; Mezyk, S. P.; Shidler, S.; Castleman, J.; Kaiser, S.; Horne, G. P. The Reactivity of Polyethylene Microplastics in Water under Low Oxygen Conditions Using Radiation Chemistry, *Water* **2021**, *13*, 3120.

25. Xu, H.; Casabianca, L. B. Probing Driving Forces for Binding Between Nanoparticles and Amino Acids by Saturation-Transfer Difference NMR, *Sci. Rep.* **2020**, *10*, 12351.

26. Xu, H.; Casabianca, L. B. Dual Fluorescence and NMR Study for the Interaction between Xanthene Dyes and Nanoparticles, *Langmuir*, **2021**, *37*, 385-390.

27. Zhang, Y.; Casabianca, L. B. Probing Amino Acid Interaction with a Polystyrene Nanoparticle Surface Using Saturation-Transfer Difference (STD)-NMR, *J. Phys. Chem. Lett.* **2018**, *9*, 6921-6925.

28. Zhang, Y.; Xu, H.; Parsons, A. M.; Casabianca, L. B. Examining Binding to Nanoparticle Surfaces Using Saturation Transfer Difference (STD)-NMR Spectroscopy, *J. Phys. Chem. C* **2017**, *121*, 24678-24686.

29. Zhang, Y.; Xu, H.; Casabianca, L. B. Interaction Between Cyanine Dye IR-783 and Polystyrene Nanoparticles in Solution, *Magn. Reson. Chem.* **2018**, *56*, 1054-1060.

30. Suzuki, Y.; Shindo, H.; Asakura, T. Structure and Dynamic Properties of a Ti-Binding Peptide Bound to TiO_2 Nanoparticles As Accessed by ^1H NMR Spectroscopy, *J. Phys. Chem. B* **2016**, *120*, 4600-4607.

31. Suzuki, Y.; Shindo, H. Binding sites and structure of peptides bound to SiO_2 nanoparticles studied by solution NMR spectroscopy, *Polym. J.* **2018**, *50*, 989-996.

32. Stephen, K.; Gayathri, V.; Lobo, N. P.; Kumar, B. V. N. P.; Jaisnakar, S. N.; Samanta, D. Improving Hydrophobicity of Collagen with Silica Nanoparticles: Probing a Noncovalent Approach, *Langmuir* **2023**, *39*, 10828-10842.

33. Tavares, W. D.; Pena, G. R.; Martin-Pastor, M.; Oliveira de Sousa, F. F. Design and characterization of ellagic acid-loaded zein nanoparticles and their effect on the antioxidant and antibacterial activities, *J. Mol. Liq.* **2021**, *341*, 116915.

34. Chen, J.; Wang, J.; Bai, Y.; Li, K.; Garcia, E. S.; Ferguson, A. L.; Zimmerman, S. C. Enzyme-like Click Catalysis by a Copper-Containing Single-Chain Nanoparticle, *J. Am. Chem. Soc.* **2018**, *140*, 13695-13702.

35. Chiodo, F.; Enríquez-Navas, P. M.; Angulo, J.; Marradi, M.; Penadés, S. Assembling different antennas of the gp120 high mannose-type glycans on gold nanoparticles provides superior binding to the anti-HIV antibody 2G12 than the individual antennas, *Carbohyd. Res.* **2015**, *405*, 102-109.

36. Dai, Q.; Du, Z.; Jing, L.; Zhang, R.; Tang, W. Enzyme-Responsive Modular Peptides Enhance Tumor Penetration of Quantum Dots via Charge Reversal Strategy, *ACS Appl. Mater. Inter.* **2024**, *16*, 6208-6220.

37. An, Y.; Sedinkin, S. L.; Venditti, V. Solution NMR methods for structural and thermodynamic investigation of nanoparticle adsorption equilibria, *Nanoscale Adv.* **2022**, *4*, 2583.

38. Perera, Y. R.; Hill, R. A.; Fitzkee, N. C. Protein Interactions with Nanoparticle Surfaces: Highlighting Solution NMR Techniques. *Isr. J. Chem.* **2019**, *59*, 962-979.

39. Meyer, B.; Peters, T. NMR Spectroscopy Techniques for Screening and Identifying Ligand Binding to Protein Receptors, *Angew. Chem. Int. Ed.* **2003**, *42*, 864-890.

40. Egner, T. K.; Naik, P.; Nelson, N. C.; Slowing, I. I.; Venditti, V. Mechanistic Insight into Nanoparticle Surface Adsorption by Solution NMR Spectroscopy in an Aqueous Gel. *Angew. Chem.* **2017**, *129*, 9934-9938.

41. Egner, T. K.; Naik, P.; An, Y.; Venkatesh, A.; Rossini, A. J.; Slowing, I. I.; Venditti, V. 'Surface Contrast' NMR Reveals Non-Innocent Role of Support in Pd/CeO2 Catalyzed Phenol Hydrogenation. *ChemCatChem* **2020**, *12*, 4160– 4166

42. Mayer, M.; Meyer, B. Group epitope mapping by saturation transfer difference NMR to identify segments of a ligand in direct contact with a protein receptor, *J. Am. Chem. Soc.* **2001**, *123*, 6108-6117.

43. Mayer, M.; Meyer, B. Characterization of ligand binding by saturation transfer difference NMR spectroscopy, *Angew. Chem. Int. Edit.* **1999**, *38*, 1784-1788.

44. Nel, A. E.; Mädler, L.; Velegol, D.; Xia, T.; Hoek, E. M. V.; Somasundaran, P.; Klaessig, F.; Castranova, V.; Thompson, M. Understanding biophysicochemical interactions at the nano-bio interface, *Nat. Mater.* **2009**, *8*, 543-557.

45. Hwang, T. L.; Shaka, A. J. Water Suppression That Works. Excitation Sculpting Using Arbitrary Wave-Forms and Pulsed-Field Gradients, *J. Magn. Reson. A* **1995**, *112*, 275-279.

46. Wishart, D. S.; Guo, A. C.; Oler, E.; Wang, F.; Anjum, A.; Peters, H.; Dizon, R.; Sayeeda, Z.; Tian, S.; Lee, B. L.; Berjanskii, M.; Mah, R.; Yamamoto, M.; Jovel, J.; Torres-Calzada, C.; Hiebert-Giesbrecht, M.; Lui, V. W.; Varshavi, D.; Varshavi, D.; Allen, D.; Arndt, D.; Khetarpal, N.; Sivakumaran, A.; Harford, K.; Sanford, S.; Yee, K.; Cao, X.; Budinski, Z.; Liigand, J.; Zhang, L.; Zhang, J.; Mandal, R.; Karu, N.; Dambrova, M.; Schiöth, H. B.; Greiner, R.; Gautam, V. HMDB 5.0: the Human Metabolome Database for 2022, *Nucleic Acids Res.* **2022**, *50*, D622-D631.

47. Hoch, J. C.; Baskaran, K.; Burr, H.; Chin, J.; Eghbalnia, H. R.; Fujiwara, T.; Gryk, M. R.; Iwata, T.; Kojima, C.; Kurisu, G.; Maziuk, D.; Miyanoiri, Y.; Wedell, J. R.; Wilburn, C.; Yao, H.; Yokochi, M. Biological Magnetic Resonance Data Bank, *Nucleic Acids Res.* **2023**, *51*, D368-D376.

48. Markley, J. L.; Bax, A.; Arata, Y.; Hilbers, C. W.; Kaptein, R.; Sykes, B. D.; Wright, P. E.; Wüthrich, K. Recommendations for the presentation of NMR structures of proteins and nucleic acids, *Eur. J. Biochem.* **1998**, *256*, 1-15.

49. Jayalakshmi, V.; Krishna, N. R. Complete Relaxation and Conformational Exchange Matrix (CORCEMA) Analysis of Intermolecular Saturation Transfer Effects in Reversibly Forming Ligand-Receptor Complexes, *J Magn. Reson.* **2002**, *155*, 106-118.

50. Angulo, J.; Nieto, P. M. STD-NMR: application to transient interactions between biomolecules – a quantitative approach, *Eur Biophys J* **2011**, *40*, 1357-1369.

Table of contents graphic: